Title
LOW-EHERGY ION ACCELERATOR FOR HOT-ATOM CHEMICAL RESEARCH

Authors
Pohlit, H. M.
Erwin, W.R.
Reynolds, F.L.
et al.

Publication Date
1970-02-01

Submitted to Review of Scientific Instruments

UCRL-19703
Preprint

c. 2

A LOW-ENERGY ION ACCELERATOR FOR HOT-ATOM CHEMICAL RESEARCH

H. M. Pohlit, W. R. Erwin, F. L. Reynolds,
R. M. Lemmon, and M. Calvin

February 1970

AEC Contract No. W-7405-eng-48

LAWRENCE RADIATION LABORATORY
UNIVERSITY of CALIFORNIA BERKELEY

UCRL-19703

DISCLAIMER

A Low-Energy Ion Accelerator for Hot-Atom Chemical Research*

H. M. Pohlit, W. R. Erwin, F. L. Reynolds, R. M. Lemmon, and M. Calvin
Laboratory of Chemical Biodynamics, Lawrence Radiation Laboratory, and
Department of Chemistry, University of California,
Berkeley, California 94720

An ion accelerator is described that delivers magnetically separated ion currents of 0.1-20 μA at 5 eV-10 KeV energy into targets of 5 mm^2. An electrostatic decelerator in front of the target permits continuous lowering of the ion energy to ca. 5 eV. The accelerator has been used mainly for the production of $^{14}C^+$-ion beams from $^{14}CO_2$ for the study of the hot-atom chemistry of carbon in solid benzene. The ion source is of all metal construction, and is a straight-capillary arc type. It delivers C^+ currents of approx. 2 μA, obtained at 0.2-0.5% efficiency from the $^{14}CO_2$ source gas.

INTRODUCTION

The opportunities for the study of molecular dynamics and, more specifically, for the chemical kinetics of "single collision" events between atomic and molecular beams, each in well defined quantum states, are widely recognized.[1] However, in view of the still severe limitations

*The work reported in this paper was sponsored by the U. S. Atomic Energy Commission.

[1] a) B. M. Mahan, Acc. Chem. Research 1, 217 (1968); b) R. Wolfgang, R. N. Zare, L. M. Branscomb, Science 162, 814 (1968).

both on the availability of desirable reactant beams and on the identification of the states of the scattered (product) beams, particularly of those from reactive collisions, experimentation on a level somewhat intermediate between single collision events and that of "ordinary" gas phase kinetics may be profitable for yet some time to come.

The present paper describes an ion accelerator designed to deliver beams of $^{14}C^{+}$ ions (but also other ions) with variable energy between 5 eV and several thousand eV to a solid organic target where the beam is totally absorbed. Because of the very large number of collisions involved in the interaction with the target, the microscopic specificity of information (otherwise available through "single collision" scattering) is sacrified. However, the products, which finally arrive at thermal equilibrium with the solid target matrix, can be readily identified by various standard techniques. In order to find micro quantities of products, it is necessary to use ^{14}C ions in the beam. This has the added advantage of enabling one to distinguish between products formed from interactions with beam particles and those formed from other events in the target matrix.

As in kinetics studies via thermal, photo, or chemical activation, great uncertainty exists with respect to the distribution of states of the actual reactants. However, the possibility in the present method of clearly defining and varying the maximum kinetic energy of the reactant over a wide chemically important range clearly offers advantages over the above methods. For the same reasons, it offers

advantages over the nuclear activation method ("hot-atom" chemistry), through which the chemical fate of originally fast atoms is frequently investigated.[2]

In the present paper we shall describe the accelerator, our long-time experience with it, and some of the research progress that has been achieved thru its use. Meninger has described similar work with accelerated T^+ and T_2^+ beams.[3]

GENERAL DESCRIPTION (see Fig. 1)

The ion accelerator of this report was first built a decade ago, but only described in laboratory reports.[4-6] Numerous modifications and improvements have been recently made, and they are emphasized in the present report.

The accelerator is mounted on an angle iron stand 40x30 in., 40 in. high; the plane of ion trajectories is horizontal. Originally, source and target were located symmetrically with respect to the 90° magnet; however, after several imaging devices were added in the target arm, the distances of source to the source-side principal plane of the magnetic field, and from the target-side principal plane to the target,

---

[2] R. Wolfgang, Progress in Reaction Kinetics 3, 97 (1965).

[3] M. A. Menzinger, Ph.D. Thesis, Yale University, 1968.

[4] F. L. Reynolds, University of California Radiation Laboratory Report No. UCRL-8618 (1959), p. 76.

[5] R. T. Mullen, Ph.D. Thesis, University of California, Berkeley, 1961, UCRL-9603.

[6] H. M. Pohlit, Ph.D. Thesis, University of California, Berkeley, 1969, UCRL-18895.

are now 51 and 93 cm respectively. The centers of the first focus, first and second cylinder lens, and decelerator lens system are located at 13, 33, 46, and 84 cm with respect to the source and target-side magnetic field principal plane, respectively.

The magnet yoke is mounted on a 1/4-in. Dural plate covering most of the upper plane of the angle iron frame. The two coils are located in the short section of the U-shaped yoke to give maximum space for accessories at and around the accelerator housing.

Two diffusion pumps are located inside the steel frame, and there are three mechanical pumps outside. Most power supplies, etc. are mounted on separate racks near the accelerator. The accelerator plus accessories take up the better part of a 300 ft^2 room.

Vacuum

A MCF 300 oil-diffusion pump (Silicone oil 704) is located near the first focus lens taking up most of the source gas load (normally ca. 10^{-8} moles/sec). A MCF 700 diffusion pump is tied into the vacuum system on the inside of the magnetic arc channel. Both diffusion pumps (combined speed 1000 liters/min at 10^{-5} Torr) are water cooled, have a water-cooled baffle, and a liquid nitrogen trap. They work against a fore-pressure of about 15 microns, supplied by two mechanical pumps on a manifold. A third pump is used for roughing. All mechanical pumps exhaust into a manifold which is vented into the general laboratory hood-exhaust system through a KOH (Ascarite) trap (or other traps according to varying requirements such as when the ion source is charged with ^{14}CO instead of $^{14}CO_2$).

The liquid nitrogen traps are filled automatically from a 150-liter storage tank. They consume about 80 liters/day. Typical pressures are: near the magnet, 3×10^{-7} Torr, in the target box, 4×10^{-6}. Such a vacuum provides an approx. 95% chance for an ion to traverse from source to target without collision with residual gas molecules.

Aluminum, stainless steel, glass, and brass have been used as materials for different parts of the vacuum house. The insulating flange separating the arc chamber from the accelerator body is made of an epoxy-fiberglass laminate (trade name "Nema FR4"). The whole flange was coated with epoxy and subsequently machined. All seals are made of Neoprene O-rings greased with Silicone high vacuum grease. Most electrical feed-throughs are of glass.

The Ion Source (see Fig. 2)

The ion source is made of stainless steel and is of the straight capillary arc type. It and its glass version have been described in a few early reports.[7-13] In most cases, however, this type has been

---

[7] M. A. Tuve, O. Dahl, and L. R. Hofstad, Phys. Rev. 48, 241 (1935).

[8] E. L. Yates, Roy. Soc. London, Proc. A, 168, 148 (1938).

[9] E. S. Lamar, W. W. Buechner, and R. J. Van de Graaff, J. Appl. Phys. 12, 132 (1941).

[10] E. S. Lamar, E. W. Samson, and K. T. Compton, Phys. Rev. 48, 886 (1935).

[11] E. S. Lamar, W. W. Buechner, and K. T. Compton, ibid. 51, 936 (1939).

[12] M. von Ardenne, Tabellen z. Angew. Physik., Bd. 1, VEB Deutscher Verlag d. Wissenschaften, Berlin, 1962.

[13] M. S. Livingston, M. G. Holloway, and C. P. Baker, Rev. Sci. Instr. 10, 63 (1939).

used for the production of high energy proton beams with 1-10% efficiency, and for carbon beams seemingly only on a trial basis.[8] Singly-charged carbon ion beams for ^{14}C hot-atom chemistry, i.e., with about 1 μA intensity, from a magnetically confined hot-filament discharge, have been reported by Aliprandi et al.[14]

The present source was chosen because it was considered, at the time of design,[4] to be the only one capable of producing a beam with sufficient intensity and with an energy spread of less than 1 eV.[15] Our measurements on C^+-ion beams from CO_2, however, show about 2-3 eV energy spread, in agreement with a statement by v. Ardenne, presumably referring to H^+ ion beams.[12]

We can confirm most of the details of capillary-arc operations that have been reported by others for different source gases. Outstanding are the arc's extreme sensitivity to the condition of the capillary's inside surface, and its low efficiency. The hot filament's reaction with the source gas may be the cause for the relatively rapid surface contamination requiring disassembly and thorough cleaning with fine abrasives and metal polish every 20-40 hr of operation. The filament, V-shaped, ca. 3 cm long tungsten wire (15 mil), spot-soldered or mechanically mounted on 12.7 cm long stainless steel rods (0.32 cm in diameter), also lasts a maximum of 20-30 hr. Other filament materials

---

[14] B. Aliprandi, F. Cacace, L. Cicri, G. Givanni, R. Masironi, and M. Zifferero, Ricerca Sci. 26, 3029 (1956).

[15] J. B. Hasted, "Charge Transfer and Collisional Detachment," in Atomic and Molecular Processes, D. R. Bates, Ed. (Academic Press, New York, 1962), p. 711.

(rhenium strip, thoriated tungsten, and tantalum wire) did not show any discernible difference in lifetime or effect upon the arc performance. The filament emits (depending on its age) about 0.5 A at 10-15 A DC heating current.

The anode consists of a hollow cylinder of either tantalum or stainless steel. However, no differences were detected between the different materials or between different shapes. At ca. 0.5 A arc current, heating of the anode is only moderate (estimated 400-500°), requiring no active cooling. The arc chamber body, however, receives cooling by insulated recirculating water, mainly to deduct heat from the filament compartment.

With anode and filament (cathode) mounted on axial activators, no differences were found in the characteristics of the arc when the distances of these electrodes from their respective capillary entrances were changed. However, the striking of the arc became markedly more difficult when the distances were increased beyond 2 cm.

Striking of the arc proceeds by raising both wall voltage and anode voltage sufficiently high, after an arc has been established between arc chamber wall and filament in the filament compartment. (All arc source voltages are referenced to one leg of the filament.) The arc gas pressure is usually somewhat above the minimum operating pressure (see Table I). In this procedure the arc chamber changes function from an auxiliary anode to a giant probe. With a sufficiently "stiff" power supply (2 A, 150 V), its potential can be varied, and it was found that greater arc stability resulted with "wall voltages" of 60-100 V, i.e., greater resistance towards arc breakage

was obtained; the latter was often caused by small discharges in the extraction region of the beam. More importantly, however, the striking of the arc was considerably easier with an independently adjustable wall voltage. Thus, with ca. 100 V and 500 mA (emission limited) between filament and wall, the arc strikes through the capillary to the anode as soon as the latter's potential is raised to 150-200 V. With accumulated heavy deposition of carbonaceous deposits, it is sometimes impossible to strike the arc. When the anode voltage is increased to 60-90 V above that of the wall, the filament-wall current decreases to zero. This is usually optimal for ^{+}C beam intensity. Further increase of the anode voltage makes the arc rather sensitive to disturbances, resulting in its breakage (see Fig. 3). This sensitivity is heightened when deposits have accumulated on the arc chamber inside or on the anode.

Both the ion beam intensity and, consequently, the efficiency increase sharply when the arc pressure is decreased (see Fig. 4). However, the tendency towards breaking also increases. This sensitivity is also a disadvantage of this type of ion source. This is particularly important for low-energy irradiations since the true energy of the ions (see below) was found to depend on arc conditions. After the arc is struck, for example, it takes 10-20 sec for the energy to stabilize. As one approaches the arc's breaking point, its sensitivity is reflected in larger energy fluctuations.

Radio-frequency oscillations have been observed for various arc parameters, and for all source gases. The frequency was always rather

constant at 0.6 MHz. However, amplitudes can range up to 5 V peak-to-peak. These high amplitude oscillations were observed to have a broadening effect upon the energy distribution; sometimes they also cause a shift towards lower energies. However, they can be avoided by slight changes of some arc parameters, without impairing either arc or output. The rf-potential of the arc chamber wall is monitored on an oscilloscope through a 1 nF, 10 KV capacitor. In the absence of rf-oscillation only a ca. 0.3 V "hash" is generated by the arc, i.e., after we had filtered out some ac ripple on the arc power supply outputs. Constant potentials in the arc are necessary for good energy homogeneity in the ion beam.

Table I shows arc conditions and ion beam output for different arc charges. It is possible, however, that efficiency and intensities can be improved for such gases as H_2 and CH_4, as little effort has been applied in this direction as yet. For CO_2 or CO the efficiency of ^+C at the target (2 μA) is about 0.2%. The flow rate is about 10^{-8} moles/sec CO_2 at 20 μ arc pressure.

We found that admixtures of He to CO_2 in ratios up to 5:1 did not make the operation of the arc much more difficult, i.e., the minimum operating pressure was about the same as for pure CO_2, while the C^+ beam intensity remained unaffected. Thus, the efficiency was increased by a factor of approximately 5. This helium effect has also been observed in other ion sources.[16]

---

[16] W. R. Arnold, Rev. Sci. Instr. 23, 97 (1952).

Variable gas mixtures in the arc chamber can be easily obtained by the use of three simultaneous, separate gas feeds to the arc chamber. Thus, the arc can be started with inexpensive argon, which is subsequently shut off when the $^{14}CO_2$ arc operating flow rate has been established. Thus, also, the expensive $^{14}CO_2$ is never actually mixed with He until it enters the arc chamber. It can be, therefore, easily and rapidly transferred into and out of special storage containers by trapping with liquid nitrogen.

All gas reservoirs are at ground potential and insulated from the arc chamber high voltage by 20 cm long, 7 mm ϕ, pyrex tubes. The reservoir pressure is chosen such that no breakdown occurs in the glass tubes (20-100 Torr for most gases). This requires that the gas flow regulating needle valves have to be at high-voltage potential (insulated handles).

Discharges occur occasionally between arc chamber body and extraction electrode. Their frequency increases as deposits form on the surfaces of the electrodes involved. The discharges are due to accumulation of positive charges on the deposits, followed by breakdown across the deposit to the respective metal surface. This discharge is the source of the electrons which are accelerated towards the arc chamber and which cause the observable discharge. The latter often extinguishes the arc. Floating the extraction electrode across ca. 500 K Ω to ground somewhat alleviates this situation. However, since the actual extraction voltage fluctuates somewhat in this procedure, the focal conditions may vary considerably. If this is not tolerable, disassembling of the accelerator and careful cleaning of all surfaces is necessary.

The Magnet

The magnet gap is a C-shaped, 90° sector. Its normal radius of curvature is 15 cm, its gap width 2.5 cm. The focus points are located, therefore, symmetrically, 17.5 cm from the field entrance plane, i.e., (because of fringe fields) 2.5 cm outside the theoretical focus points.

The magnet current is supplied by an Electronic Measurements Model C633 current power supply (0-300 μA), with a current stability of 1 mA in 300 mA. At 300 mA the field strength in the center of the magnet poles is about 3400 gauss. The field stability is better than 1 in 300 gauss per hour.

Focusing Devices

Imaging takes place in the acceleration gap, the first focus electrode, the magnet, the 2-cylinder lenses, and the decelerator.

The imaging effects of the arc plasma sheath are widely recognized. They, and the general field geometry, require that the acceleration (or, more precisely, extraction) voltage be in the range of 2-10 KV, ordinarily established by the potential of the arc chamber. However, the final ion energy need not be that high if the first extraction electrode is put on appropriate negative high voltage so that the difference between it and that of the arc chamber is still sufficiently large for efficient focusing (see Fig. 5). Since deceleration takes place between extraction and first focus electrode, a lower energy ion beam, with inferior optical properties, is produced. We found that, to obtain target beams in the range of 10 eV and less, it was more practical to decelerate a high energy beam (4-6 KeV).

Differences in the shape of the extracting electrode and in the distance from the arc chamber body did not seem important. A 90° stainless steel cone with a 3 mm ϕ arc side aperture opening to a 1.5 cm straight bore, with an approx. 2 mm gap between it and arc chamber, proved most suitable with respect both to beam transmission and to minimizing the accumulation of deposits on the arc side surface.

The first focus electrode (the "spherical lens" of Fig. 1) consists of two coaxial cylinders (the inner ϕ = 3.5 cm, 4 cm long, the outer ϕ = 7.5 cm, 10 cm long). The outer cylinder is grounded and the inner is at 0.8-0.95 of the acceleration voltage, permitting focusing over a distance from 10 cm to infinity.

The 90° sector magnet acting as cylinder lens, in connection with the first focus lens, produces a one-dimensional image of the source at a target at any distance. However, for deceleration with high transmission, a circular beam is required. Therefore, an electrostatic cylinder lens at right angle to that represented by the magnetic field was added (see Fig. 6). A second similar cylinder lens, again at right angle to the first, improved the overall transmission for decelerated beams significantly.

The undecelerated beam profile (measured with a long rod electrode) of a $^{12}C^{+}$ beam at the target is shown in Fig. 7. Under deceleration, the profile widens considerably for energies less than 200 eV. However, since our targets are ca. 1 cm in diameter, this is no serious limitation. Fig. 8 shows the total $^{12}C^{+}$-ion current reaching the target through a 1.5 cm ϕ masking orifice versus deceleration potential.

The decelerator consists of 10 parallel orifice plates (i.d. 12.5 mm, o.d. 38 mm, 1/16-in stainless steel; distance between plates: 9.5 mm). The entrance aperture is 19 mm ϕ and grounded, and exit aperture (ϕ 19 mm, 3 cm from the target) is at the potential of the target box and target (see Fig. 9). The potential of the remaining 8 plates can be independently adjusted via voltage dividers, and the following (not very critical) set of values for deceleration of a 4000 eV beam to less than 10 eV was found to yield good transmission: 3.2, 3.3, 3.4, 3.55, 3.65, 3.65, 3.4, 3.99 KV. Since the arc anode potential proved a good "energy" reference (see "Energy calibration"), it was also used as a reference for the target potential.

Of importance to the hot-atom chemistry in the target (see "Experiments") is the rate of accidental neutralization of ions in the decelerator, since it may occur at higher than the final energy, and since these high-energy atoms may well be collected at the target. A check for incorporation of ^{14}C and a product analysis after an irradiation with 7 eV ions, however, with the target at +30 V counter potential, admitting only atoms into the benzene, showed that approximately 10% of the original beam had been neutralized. However, the energy of the atoms was very low ($\sim$ 10 eV), as indicated by the product analysis.

Beam Alignment

Good beam alignment with the decelerator lens is essential for good transmission. Most critical in this respect is the alignment of the arc chamber exit hole with the extraction electrode orifice. To correct for possible misalignment or shifts during operation, three sets of four-way deflectors are available. The first follows directly

after the first focus electrode. The second is provided by the two pairs of parallel inner electrodes of the electrostatic cylinder lenses, and the third by splitting decelerator plates #8 and #9 in halves at right angles. The voltage at the corresponding pairs of plates is adjustable continuously between ±300 V, symmetrically with respect to the potential of the particular units (ground for the first, positive high voltages for the 2nd and 3rd deflectors).

Energy Calibration

The beam energy and energy distribution were determined via total retardation in a Faraday cage (see Fig. 10), ~~in which the sketch is approximately to scale~~. The 3.5 KV plate was necessary to prevent secondary electrons from reaching the Faraday cage. The fall-off curves were recorded on an X-Y recorder floating on the acceleration potential (4000 V). Small X displacements ("energy") were obtained by voltage dividing of a ±45 V battery on a 10-turn helipot. The current was measured as voltage drop across a 100 K Ω, 1% resistor. Both X and Y recorder inputs were preamplified by Keithley Model 220 VTVM's.

It was first discovered that the medium beam energy shifted over a range of 20-50 V above acceleration voltage if the latter was tied to the arc chamber body (wall). The shifts depended on arc conditions but mainly on the difference between wall and anode voltage. After we connected the acceleration voltage to the anode the medium energy appeared stable within 1-2 eV, and fall-off curves such as those shown in Fig. 10 were obtained. The apparent energy distribution, dI/dV, was obtained by graphical differentiation of the fall-off curve. The true beam energy is ca. 2 eV below acceleration voltage. However, this

shift depends somewhat on the state of the inside surfaces of arc chamber and anode. This state of affairs introduces some additional uncertainty into the true energy, and perhaps an energy monitor will have to be installed if a more stable ion source does not become available.

It is difficult to determine the resolution of the energy spectrometer. It was designed to comply as best as possible with requirements described by J. A. Simpson.[17] If low resolution contributed to the apparent energy distribution, the latter should decrease or increase if the initial beam energy is lowered or raised. A variation from 2 to 6 KV, however, did not change the apparent energy width which would therefore have to be attributed to the intrinsic energy spread of the beam of 2-3 eV. This may be due to the ion source or the mechanism of C^+-ion formation. While this figure appears to be close to one reported for H^+,[12] the above conclusion is insecure because the optical properties of the 2 KeV beam are rather different from those of a 6 KeV beam. However, the energy is estimated as accurate within ± 2 eV.

We failed to achieve higher energy accuracy and control by defining the energy by the magnetic field strength and the beam trajectory. Because of the finite source size (0.6 mm ϕ), and therefore its finite image size at an energy discriminating slit near the exit face of the magnet, a large intensity loss would have to be accepted if a resolution of ca. 1 in 4000 eV were required. Slit widths of less than 0.04 mm would be required. Therefore, only the

---

[17] J. A. Simpson, Rev. Sci. Instrum. 32, 1283 (1961).

right and left edge of the source image were intercepted by a slit permitting >95% of the beam intensity to pass through. The difference current to the two intercepting slit sides was used as signal for high or low energy deviation. Its voltage, amplified (Analog Devices 180, loop gain about 200,000), was used to drive the accelerating voltage power supply (500-6000 V, John Fluke Model 408-A/U). While this energy regulator was stable, and showed a wide regulation range, the beam geometry (i.e., trajectory and profile) was not stable enough. Therefore, large energy variations were induced on account of trajectory changes. Most important, again, seemed the position of the first focal point in the acceleration gap. For instance, small shifts of the arc cathode apparently changed the position of this focal point and the trajectory so much that energy shifts by 30-40 eV were caused by the "energy regulator".

The Target

a) The sample

The standard target is a 7 x 7 cm square which forms one side of a hollow regular cube of stainless steel (see Fig. 1). The inside can is filled with coolants, usually liquid nitrogen. This target is electrically insulated from the surrounding aluminum target box (about 13 x 16 x 16 cm) so that target currents can be measured via voltage drop across a 100 KΩ resistor. The target box is insulated from the rest of the accelerator by a Corning glass pipe (38 cm i.d., 25 cm long) to permit free floating at deceleration potential.

The sample (benzene) is deposited on the cooled target surface through four (ϕ 0.4 mm) stainless steel tubes at about 1 cm distance

from the target surface and from each other. These tubes are jointly fed from the vapor space above a 2-ml graduated liquid benzene reservoir. Benzene vapor flow is rgulated by a Hoke Model TLY 442 bellows metering valve. Depending on tne nozzle spacing, the benzene is deposited within a circle of ca. 1 cm ϕ. Normal flow rates are 1-2 x 10^{-3} moles/hr. Very much larger flow rates often cause highly irregular growth of the solid.

After the irradiations are completed, the sample is transferred into vials via vacuum transfer, or in the solid state by scraping off the solid from the still-cold target in a dry nitrogen atmosphere.

b) Charge neutralization

Because of the insulating properties of solid benzene, care has to be taken of the accumulation of positive charges. Occasional electrical breakdown is caused by these charges. However, as it is preceded by an increase of the electrical potential of the target (benzene), the retarding effects are serious at energies below ca. 1500 eV. For low energy ion incorporation the positive charges are neutralized at the target surface by a commensurate flow of electrons from a hot filament of a flashlight bulb (G.E. No. 13). The emission is set so that the electron current is only space charge limited. Even then a finite "over potential" remains on the target on account of the finite perveance of the system filament-target. In order to estimate this additional retarding potential, the perveance for a filament at 1 cm distance from the straight metal target was determined to be 0.5 μA $(\text{volts})^{-3/2}$. The additional retarding potential may, therefore, be as

large as 7 V at a beam intensity of 1 μA. To minimize this energy uncertainty, the filament is kept as close as possible to the solid benzene surface.

c) Monitoring devices

By measuring the electron current (voltage drop across a 100 KΩ, 1% resistor) on a battery powered, floating VTVM (Keithley 200B), the positive ion beam intensity can be monitored. The energy of the ion beam at the target is monitored by measuring the potential difference between the arc anode and the target box with the same VTVM. It would be more important, however, to monitor the potential of the target surface. This cannot be done at the present time.

d) State of the beam ions

Because of the many collisions of the fast carbon ions or atoms in the target, which could change the distribution over various electronic states considerably, the question as to the initial state of the beam ions is not very pertinent. A survey of the possible reactions in the arc leading to C^+ from CO_2 suggests that the C^+ ion is in its electronic ground state; however, it may have a kinetic energy of formation of up to 1 eV.[6] Although this is somewhat less than the experimentally determined energy spread in the beam, it may be its main cause. An ion source with a smaller energy spread would therefore be of little advantage.

EXPERIMENTS

For results and detailed descriptions of hot-atom chemical experiments with this accelerator, see refs. 5,6, and 18-21.

Irradiations take from 1-5 hr, depending on the purpose. A 1 μA $^{14}C^{+}$ beam deposts ca. 2 μC per hr at the target. This amounts to about 4 x 10^4 dpm in a product whose yield is 1%.[20,21] For chemical degradations of these products by which the ^{14}C distribution is determined, one usually requires more activity, depending on yield and activity incorporation in the degradation products.[20,21]

In some of our irradiations we partially neutralized the $^{14}C^{+}$ ion beam by charge exchange at 5 consecutive tungsten wire grids (ϕ 1 mil, 10 mil spacing) at the entrance to the target box. Thirty percent conversion was obtained, the remaining ion beam was electrostatically deflected upon a second target. This experiment showed the equivalence of atom and ion beams, as far as the hot-atom chemistry is concerned, if the energy is larger than 500 eV. It is also a good indication that the chemically important species is, as has been widely postulated, the neutral carbon atom.[2,6]

ACKNOWLEDGMENTS

We owe thanks to many who have helped by advice and skillful work: Dr. Maynard Michel, Fritz Woeller, Pete Dowling, Del Coleman, Dick O'Brien, Robert Creedy, and Reed Johnson.

---

[18] H. M. Pohlit, T. H. Lin, W. Erwin, and R. M. Lemmon, J. Am. Chem. Soc. 91, 5421 (1969).

[19] H. Pohlit, W. Erwin, T. H. Lin, and R. M. Lemmon, submitted to J. Phys. Chem. (1970).

[20] H. M. Pohlit, T. H. Lin, and R. M. Lemmon, J. Am. Chem. Soc. 91, 5425 (1969).

[21] H. M. Pohlit and R. M. Lemmon, submitted to J. Chem. Phys. (1970).

The work described in this paper was performed under the auspices of the U. S. Atomic Energy Commission.

TABLE I

Typical Arc Conditions[1)]

Gas	AV	AC	WV	WC	P	P_{break}	P_{strike}	Major Ion Beams[2)] (μA)	Remarks
He	60	360	0	0	300	110	300	He^+:10	
Ne[3)]	60	350	0	0	50	17	45	Ne^+:10	The WC increases to 700 shortly before striking
Ar	50	360	0	50	8	5	15	Ar^+:20	
Xe	30	360	0	20	5	1	5	(>20)[4)]	
H_2/Ar(1:1)	50	360	0	0	20	15	20	H^+:0.5; H_2^+:1; H_3^+:0.3	
N_2	50	300	0	0	45	17	50	N^+:2; N_2^+:15	
O_2	65	300	0	0	60	50	100	O^+:1; O_2^+:15	
Cl_2	600	300	100	300	60	40	60		
CO_2	50	350	0	0	25	20	40	C^+:1-2; O^+:1; CO^+:15; CO_2^+:5	
CO	70	360	0	0	15	15	30	C^+:1-2; O^+:1; CO^+:15	
CH_4	80	300	100	200	170	150	170	H^+:1; H_2^+:3; H_3^+:1; C^+:0.1; CH^+:0.5; CH_2^+:1; CH_3^+:2; CH_4^+:5	
HC≡CH	50	350	0	0	30	15	40	CH^+:0.3; M_{24-26}:10	These conditions for 1:1 Ar/CH_2Cl_2; pure CH_2Cl_2: P_{strike}: 100 μ; however, no stable arc resulted.
CH_2Cl_2	50	350	0	0	30	15	20		

AV = Arc voltage (V)
AC = Arc current (mA)
WV = Wall voltage (V)
WC = Wall current (mA)
P = Pressure (μ) at which intensity of ion beams is determined.

1) These are operating conditions. Conditions before striking of arc: WV, 100V; WC, 500 mA; P, P_{strike}; AV, 300-700V; AC, 0.

2) Estimated from e/m scans behind the discriminator slit (Figure 1) 0.3 mm wide, at arc conditions as indicated.

3) "Spark chamber gas", contains 10% He.

4) At 4000V acceleration, maximum mass to pass through discriminator slit, at 3500 gauss: ca. 50.

FIGURE CAPTIONS

Fig. 1. Schematic Drawing of 10-KV Ion Accelerator.

Fig. 2. Arc Chamber, schematically.

Fig. 3. Arc Operating Characteristics for Different States of the Arc Chamber Surface and for Different Arc Atmosphere Pressures.

Fig. 4. Approximate $^{14}C^{+}$-beam Intensities at the Target Versus Arc Atmosphere Pressures.

Fig. 5. Total Usable Ion Beam Versus Ion Energy at Different Total Extraction Voltages.

Fig. 6. Electrostatic Cylinder Lens. The four outer electrodes are at ground potential, the inner at ca. 25% of the acceleration potential.

Fig. 7. Beam Profile at Target (4000 eV, $^{12}C^{+}$). Upper: horizontal scan; lower: vertical scan.

Fig. 8. Decelerator Lens Performance. The low maximum current (0.6 μA) is accidental. The ordinate can be scaled for at least 2 μA maximum current.

Fig. 9. Decelerator Lens System.

Fig. 10. Fall-off Curve, Mean Energy, and Energy Distribution of 4000 eV $^{12}C^{+}$-ion Beam.

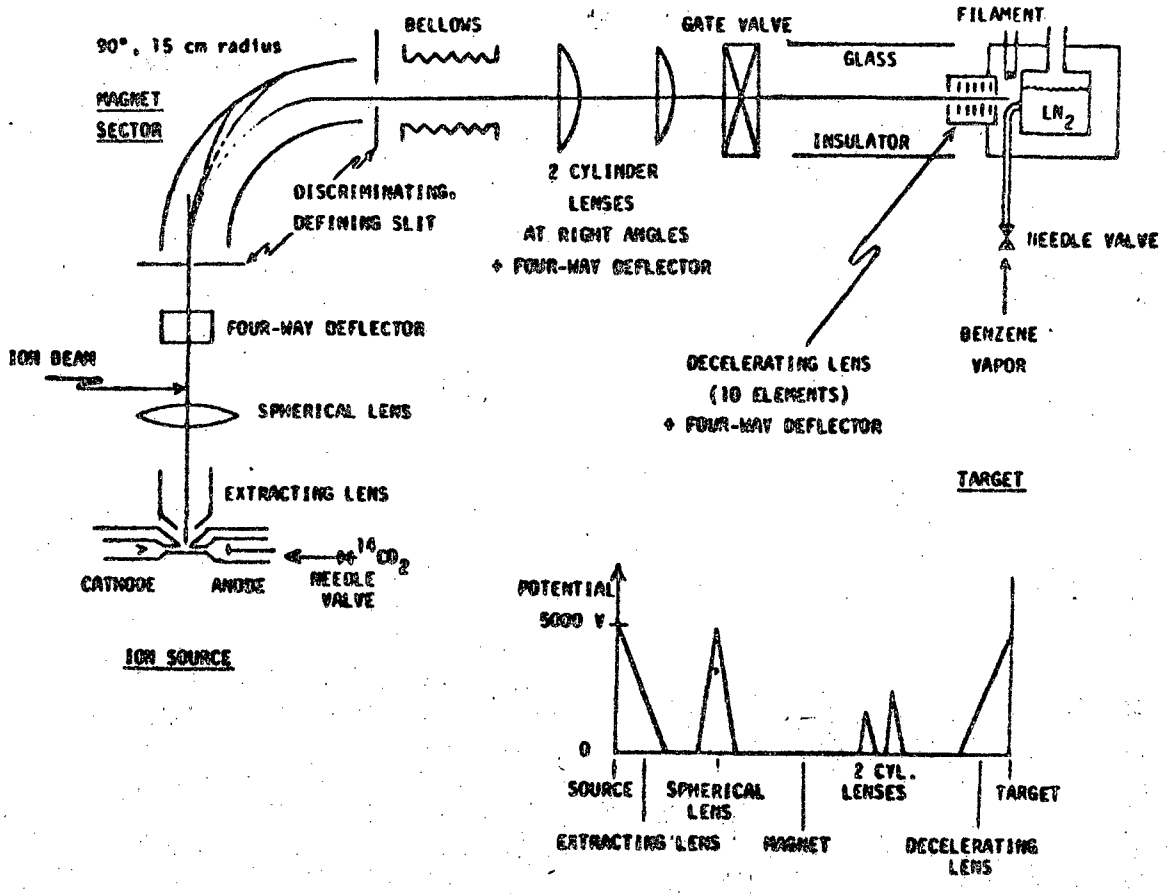
90°, 15 cm radius
MAGNET SECTOR
BELLOWS
GATE VALVE
FILAMENT
GLASS
INSULATOR
LN_2
DISCRIMINATING DEFINING SLIT
2 CYLINDER LENSES AT RIGHT ANGLES + FOUR-WAY DEFLECTOR
NEEDLE VALVE
FOUR-WAY DEFLECTOR
ION BEAM
SPHERICAL LENS
DECELERATING LENS (10 ELEMENTS) + FOUR-WAY DEFLECTOR
BENZENE VAPOR
TARGET
EXTRACTING LENS
$^{14}CO_2$
CATHODE
ANODE
NEEDLE VALVE
ION SOURCE
POTENTIAL
5000 V
0
SOURCE
SPHERICAL LENS
2 CYL. LENSES
TARGET
EXTRACTING LENS
MAGNET
DECELERATING LENS
XBL 691-4085

Fig. 1

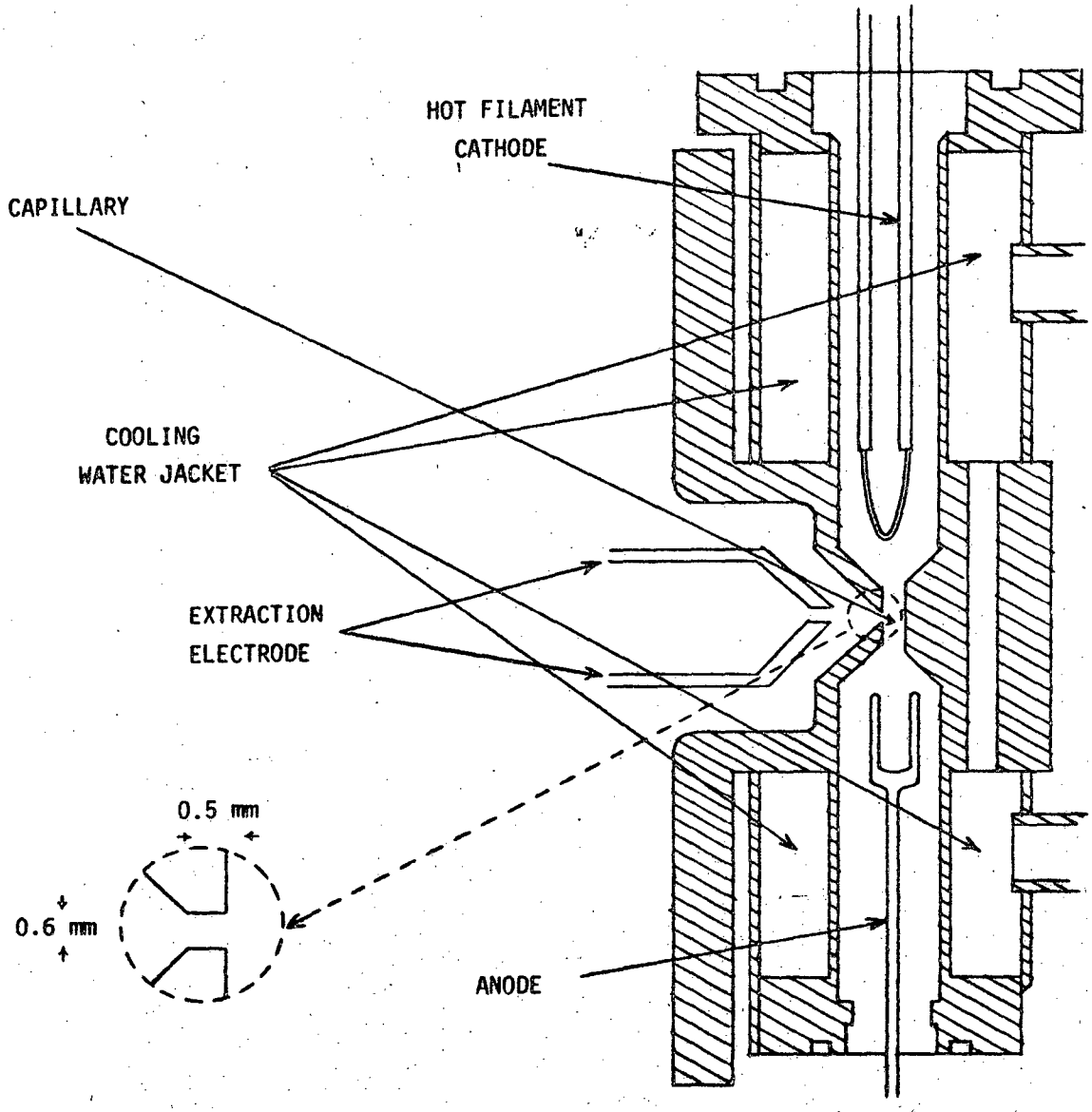

XBL 695-4231

Fig. 2

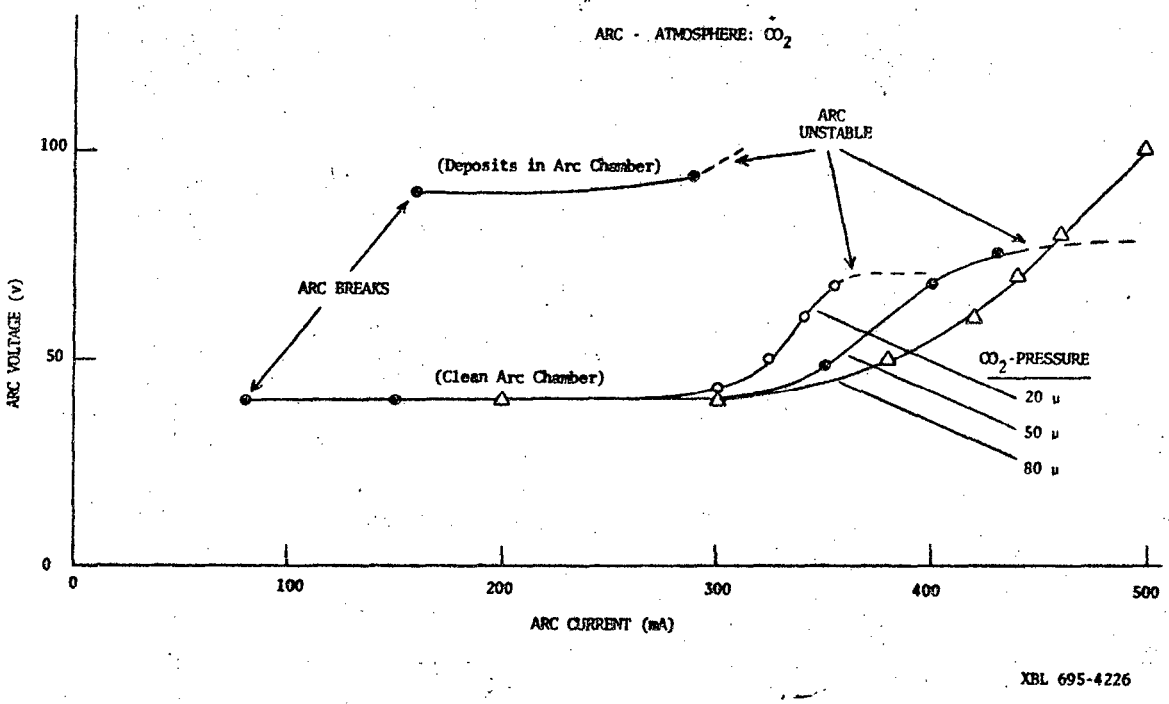
ARC - ATMOSPHERE: CO_2
ARC UNSTABLE
(Deposits in Arc Chamber)
ARC BREAKS
(Clean Arc Chamber)
CO_2-PRESSURE
20 μ
50 μ
80 μ
ARC VOLTAGE (v)
100
50
0
0
100
200
300
400
500
ARC CURRENT (mA)
XBL 695-4226

Fig. 3.

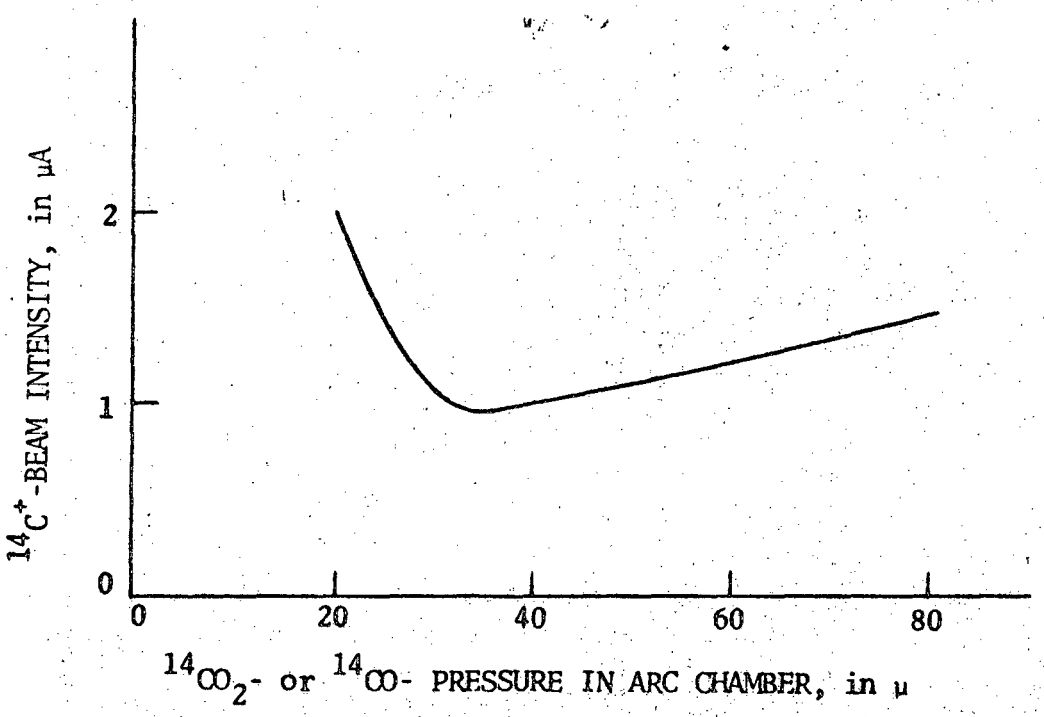

XBL 695-4228

Fig. 4

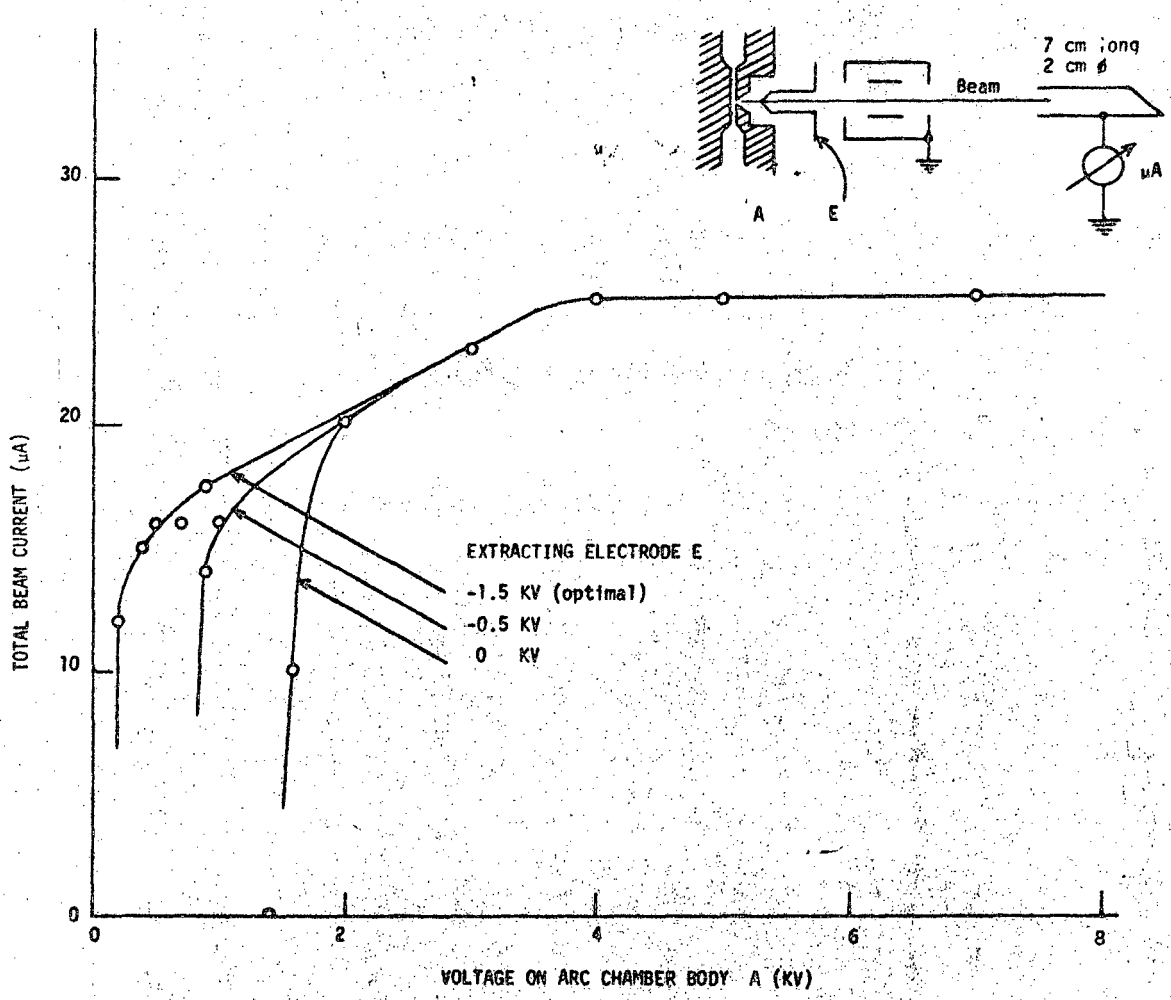

XBL 695-4248

Fig. 5

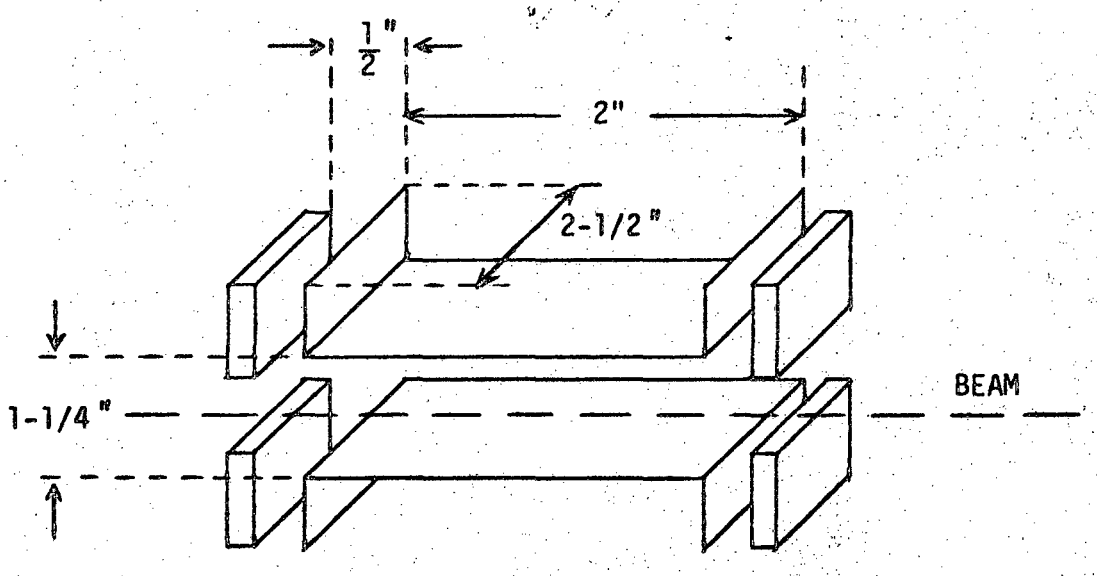

XBL 695-4255

Fig. 6

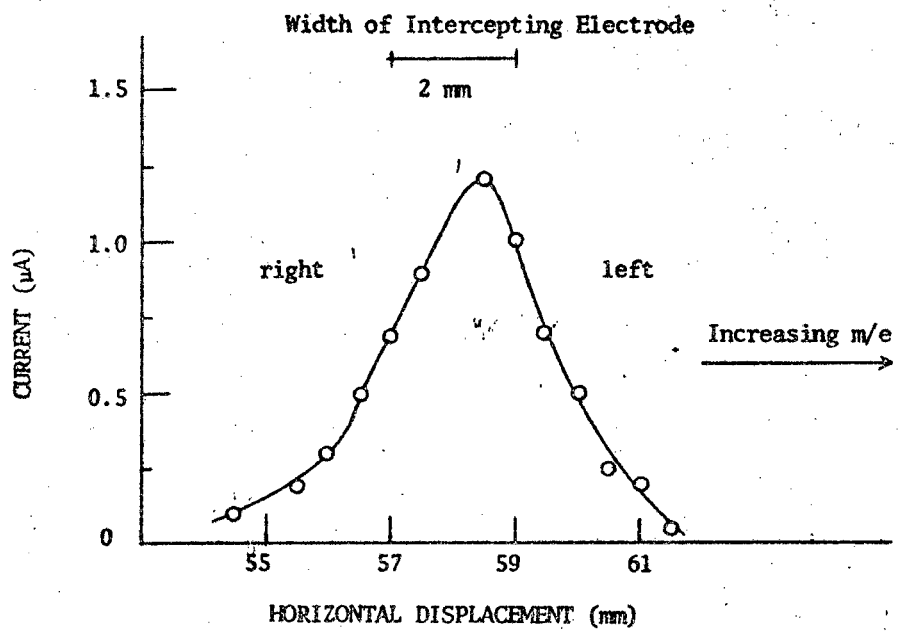

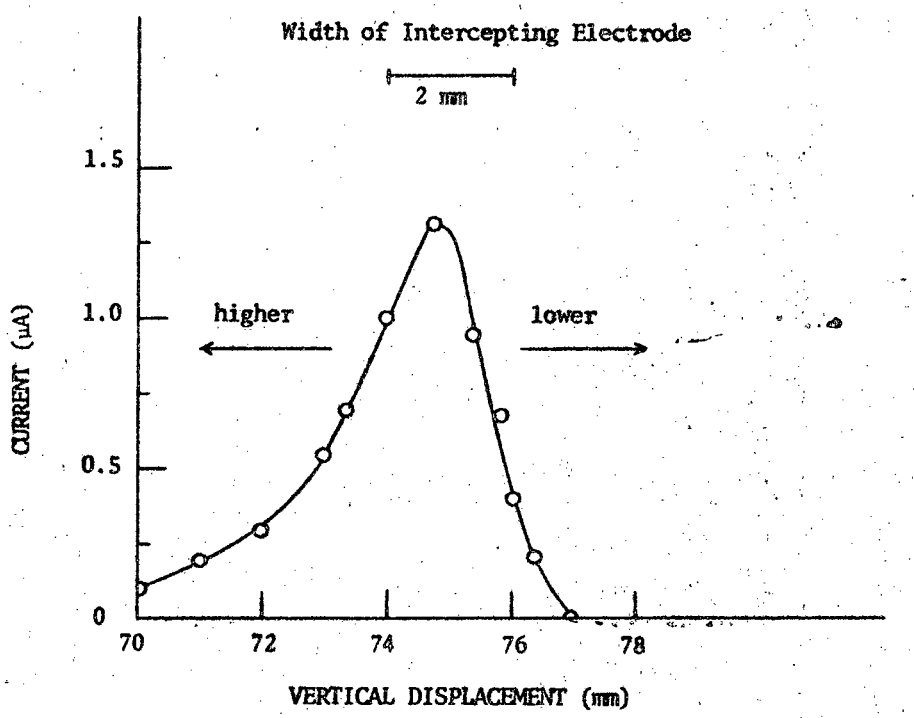

XBL 695-4225

Fig. 7

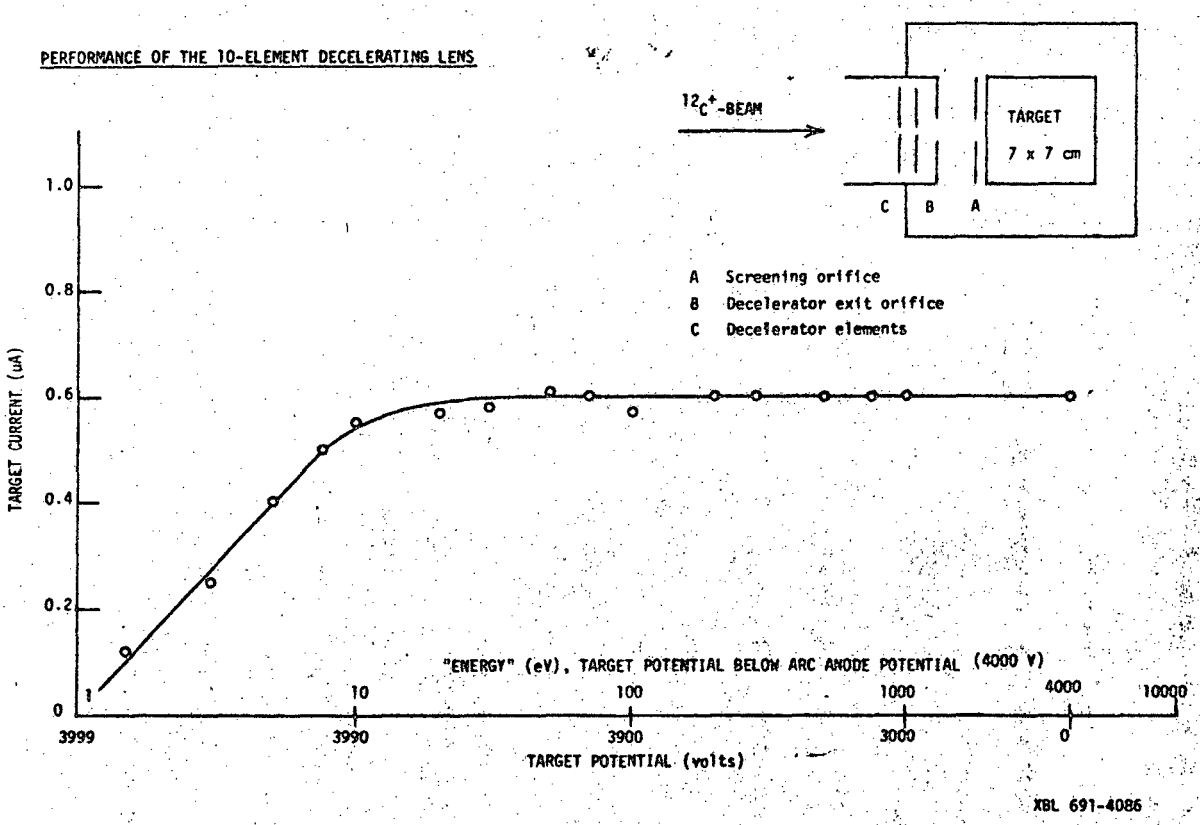
PERFORMANCE OF THE 10-ELEMENT DECELERATING LENS
$^{12}C^{+}$-BEAM
TARGET
7 x 7 cm
C
B
A
A Screening orifice
B Decelerator exit orifice
C Decelerator elements
TARGET CURRENT (μA)
1.0
0.8
0.6
0.4
0.2
0
"ENERGY" (eV), TARGET POTENTIAL BELOW ARC ANODE POTENTIAL (4000 V)
1
10
100
1000
4000
10000
3999
3990
3900
3000
0
TARGET POTENTIAL (volts)
XBL 691-4086

Fig. 8

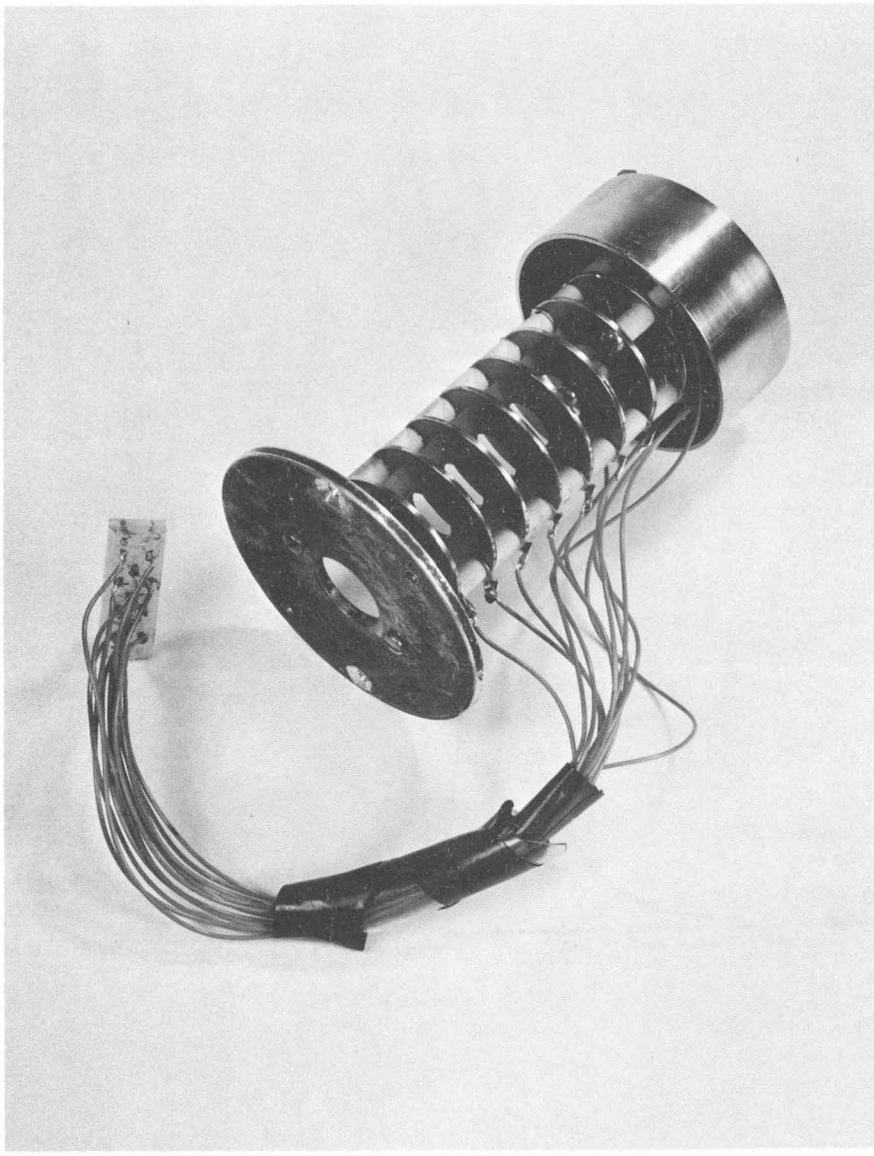

XBB 691-641

Fig. 9

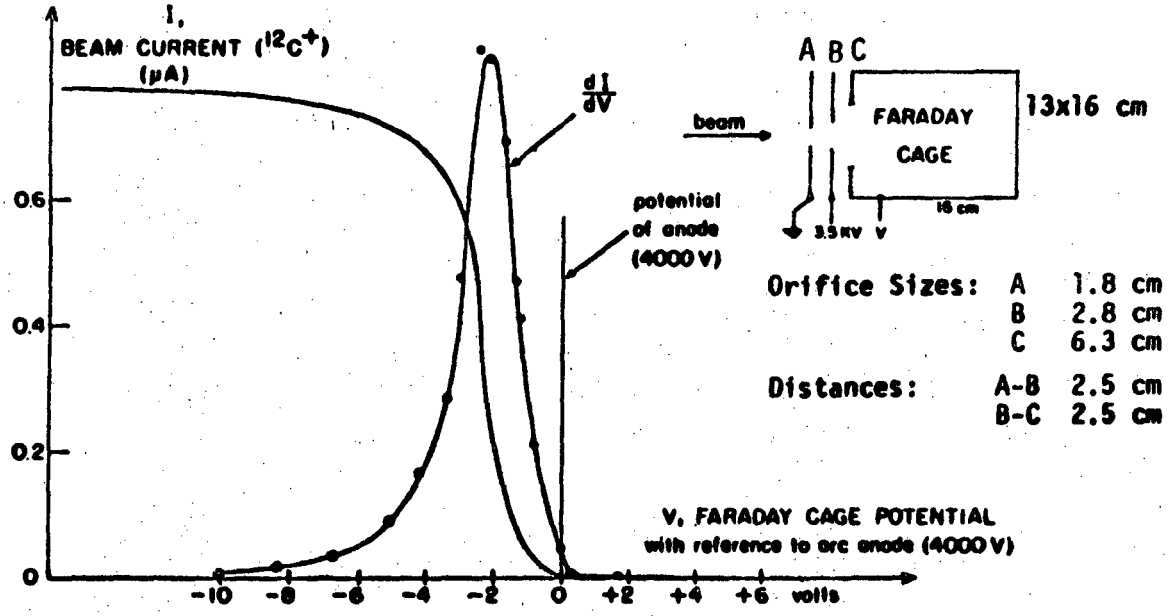

XBL 695-4253

Fig. 10

LEGAL NOTICE

TECHNICAL INFORMATION DIVISION
LAWRENCE RADIATION LABORATORY
UNIVERSITY OF CALIFORNIA
BERKELEY, CALIFORNIA 94720